Original Article

Failure Analysis: Enamel Fracture after Debonding Orthodontic Brackets

Chen-Sheng Chen[a]; Ming-Lun Hsu[b]; Kin-Di Chang[c]; Shou-Hsin Kuang[d]; Ping-Ting Chen[e]; Yih-Wen Gung[c]

ABSTRACT

Objective: To determine the location and size of enamel fracture (EF) when debonding a bracket.

Materials and Methods: Tests on actual EF situations were conducted in different debonding load modes (tension, shear, and torsion) via mechanical testing, finite element model (FEM) analysis, and scanning electronic microscopy (SEM). Through these simultaneous analyses of the relationships among debonding load modes, value/distribution of stress, and actual enamel fracture location/size, an investigation was undertaken to explore the complex failure mode during enamel fracture after debonding of an orthodontic bracket.

Results: The EF usually was located in the area where the force was exerted during various loading modes. The tensile, shear, and torsion debonding modes produce EF sizes and incidences with no significant differences. Findings on FEM matched the mechanical testing and SEM results.

Conclusions: The EF locations coincided with the areas where the tensile, shear, or torsion force was exerted. Therefore, the dentist should give extra care and attention to these specific areas of enamel after debonding. The sizes and incidences of EF produced by these three debonding modes showed no significant difference. Thus, clinically, when the sizes and incidences of produced EF are considered, it should not matter which of these three exerting forces is used to debond a bracket.

KEY WORDS: Orthodontic bracket; Debonding; Enamel fracture; Mechanical test; SEM; Finite element model

INTRODUCTION

When the orthodontic bracket is debonded, not only do some adhesive remnants remain on the enamel surface, but enamel fracture (EF) or enamel detachment may occur at the moment of debonding.[1–3] This type of EF causes stain and plaque accumulation on the rough fractured surface. Therefore, we were interested in determining the best approach to debonding the bracket to minimize the creation of EF.

Several studies have focused on the stress distribution of an enamel/adhesive/bracket interface during different loading modes, but no comprehensive survey about EF areas located, measured, or predicted has been performed to gain an understanding of the complex failure mode after a bracket is debonded. One study found that the shear mode was safer for debonding brackets than was the tension mode.[4] It also has been shown that stress distribution across the enamel/adhesive interface is far from homogeneous, and that the shear mode can cause cohesive failure.[5] A scanning electron microscopy (SEM) study of the shear bond strengths of metal brackets bonded with adhesives revealed that failure predominantly occurred at the enamel/adhesive interface.[6] When the bond strength of various bracket base designs was examined, it was also found that most debonding interfaces are located at the bracket/adhesive interface and at the enamel/adhesive interface—not within the adhesive.[7] In addition to shear, twisting force often is used to debond brackets. One study has found that when a twisting action was used to remove orthodontic brackets, EF occurred more frequently than when the

[a] Associate Professor, Department of Physical Therapy and Assistive Technology, National Yang-Ming University, Taipei, Taiwan; Taipei City Hospital, Taipei, Taiwan.

[b] Associate Professor, School of Dentistry, National Yang-Ming University, Taipei, Taiwan.

[c] Lecturer, School of Dentistry, National Yang-Ming University, Taipei, Taiwan; Department of Dentistry, Taipei City Hospital, Taipei, Taiwan.

[d] Department Head, Department of Dentistry, Taipei Veterans General Hospital, Taipei, Taiwan.

[e] Graduate Student, Institute of Rehabilitation Science and Technology, National Yang-Ming University, Taipei, Taiwan.

Corresponding author: Dr Yih-Wen Gung, School of Dentistry, National Yang-Ming University, 155 Li-Nong Street, Section 2, Shih-Pai, Taipei, Taiwan 11221
(e-mail: gung@ym.edu.tw)

Accepted: February 2008. Submitted: September 2007.

shear mode was used.[8] Few studies have taken advantage of SEM technology to measure the EF area, although SEM has been used to produce an adhesive remnant index after bracket debonding.[3,9]

It is proposed here that it should be possible to use SEM in combination with image software analysis to locate and measure EF areas. Mechanical testing ought to provide the debonding force, and finite element model (FEM) analysis should reveal the stress distribution. Modes of debonding loads, debonding force values, distribution of EF stress, and quantification and location of actual EF areas are closely related factors that should be examined and discussed together when one is attempting to understand failure modes.

Thus, in this study, we made use of three tools—mechanical testing, SEM, and FEM—to investigate these linked EF-related issues. In addition, we used statistics to identify useful correlations between these issues. Therefore, this study was designed to measure all of these factors and to evaluate the areas of EF in relationship to the various debonding force modes used. In a clinical setting, dentists should be able to use the results of this study to reduce the likelihood of EF when debonding brackets.

MATERIALS AND METHODS

Mechanical Testing

Thirty human premolar specimens with intact enamel surfaces were collected, and 30 stainless steel standard edgewise orthodontic premolar brackets (Tomy International Inc., Tokyo, Japan) were chosen for the debonding tests. Extracted premolar specimens were stored at room temperature in distilled water, which was changed every day before bonding.[6] The teeth were used within 3 months after extraction.[10]

The surface enamel was cleaned, etched, and primed (Transbond XT; 3M Unitek, St Paul, Minn) according to the manufacturer's instructions. A Teflon tape with a hole in the center was placed onto the treated tooth surface to standardize the bonding region[10] to a constant area of 9.9 mm^2. The dimension of the hole was the same as that of the bracket base. Then the bonding region of enamel was primed with 0.001 g primer (Transbond XT). The bonding base of the bracket was applied with resin adhesive (Transbond XT); then the bracket was positioned and pressed onto the restricted hole region of enamel with 250 g force for 5 seconds to ensure uniform adhesive thickness.[11] Excess adhesive was removed from the margin of the bracket, first with a tip of the probe, then by microbrushing (Kerr, Orange, Calif). The light-cure adhesive was exposed to halogen light (Optilux 501; Kerr) for 20 seconds by shining the light for 10 seconds each on the mesial side and the distal side. Each bonded specimen was embedded in a cylindrical die-stone block (Die-Keen; Heraeus Kulzer GmbH & Co., KG, Hanau, Germany) with the crown exposed. Bonded specimens were stored in water at 37°C for 24 hours prior to testing.[12]

The specimens were randomly divided into three groups of 10. Specimens in one group were brought to failure under the tension mode, specimens in the second group were brought to failure under the shear mode, and specimens in the third group were brought to failure under the torsion mode (Figure 1A). An MTS Mini Bionix 858II (MTS System Corporation, Eden Prairie, Minn) was used to apply force to the specimens. The tensile force was exerted from the corners of the bracket. Because of MTS shear mode design limitations, the shear force was exerted from the mesial side to the distal side. Shear mode and tension mode tests were performed at a crosshead speed of 1 mm/min.[9,13,14] The specimens under torsion mode were subjected to torsion at a velocity of 10 degrees/min. Descriptive statistics were calculated for each of the three groups of teeth tested. An independent *t*-test was used to determine whether differences between the forces needed to debond the brackets were significant between the tensile mode group and the shear mode group. Significance was predetermined at $P = .05$.

SEM

After failure, the specimens were mounted on aluminum stubs, and sputter was coated with approximately 15 to 20 nm of a gold palladium mixture. The fracture surfaces were photographed with the use of a JEOL SEM machine (JSM-T100; JEOL Ltd., Tokyo, Japan) operated at 15 kV. Areas of EF were identified and measured with Optimas 6.5 image software (Image Processing Solutions Inc., North Reading, Mass) (Figure 1B), and the contact area of the orthodontic bracket was measured at 9.9 mm^2. The EF percentage was derived by dividing the EF area by 9.9 mm^2. Additionally, the EF sites were located and mapped into 3×3 matrix boxes. To understand whether the size of EFs produced was related to the three loading modes, both one-way analysis of variance (ANOVA) and the Kruskal-Wallis test were performed. Data without inclusion of the 0 values of EFs were analyzed via ANOVA testing. Data that included the 0 values of EFs were analyzed by means of the Kruskal-Wallis test. Also, pairwise comparisons using Fisher's exact tests with Bonferroni correction were performed to examine whether the difference in incidence of EFs among the three groups was significant. Significance was predetermined at $P = .05$.

FEM

To analyze stress distribution, an FEM comprising three materials—enamel, adhesive, and bracket—was

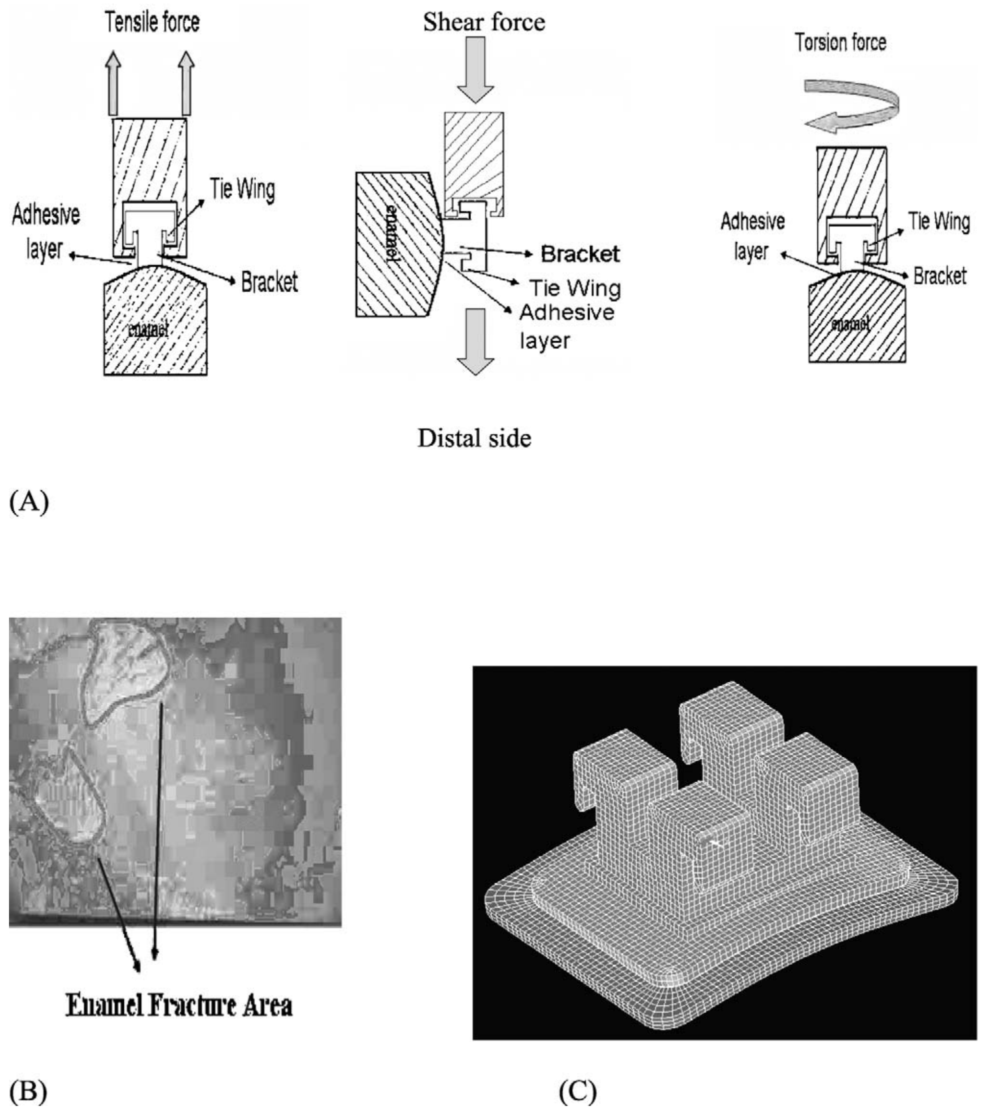

Figure 1. (A) Different loading modes for debonding an orthodontic bracket. (B) Identification of the enamel fracture (EF) area under scanning electron microscopy (SEM). (C) The finite element model (FEM) consisted of 31,255 nodes and 21,216 elements.

constructed with the use of ANSYS 7.0 software (Swanson Analysis System Inc., Houston, Tex). This FEM consisted of 31,255 nodes and 21,216 solid elements. Its material properties were adopted from a previous study[8] in which Young's modulus and the Poisson ratio were defined at 210,000 MPa and 0.3, respectively, for the orthodontic bracket; 11,721 MPa and 0.21, respectively, for the adhesive; and 46,890 MPa and 0.3, respectively, for the enamel.

This model was assumed to be isotropic, homogeneous, and linear elastic. The model configuration was based on the experimental test setup. Because this study investigated only the interface between enamel and adhesive, the enamel was only partially created and the bottom of the enamel was completely fixed (Figure 1C). The magnitude and location of the loading conditions were modeled on the basis of mechanical testing results. In this study, we evaluated enamel stress distribution by examining the principal stress. For the three principal directions, we regarded the maximum principal stress as an evaluation index, because the character of enamel material is close to that of a brittle material.

Stress Evaluation in FEM

Finite element formulation usually results in a continuous displacement field from element to element—not a discontinuous stress field. As a result, to obtain more accurate stresses for the model, this study used a strain energy error to evaluate the stress error; this approach was based on the study findings of Zienkiewicz and Zhu.[15] The stress evaluation process proceeded as follows[16]:

$$\{\Delta\sigma_n^i\} = \{\sigma_n^a\} - \{\sigma_n^i\}$$

Table 1. Debonding Force and Enamel Fracture Measurement in Different Loading Modes[a]

Loading Mode	Specimen No.	1	2	3	4	5	6	7	8	9	10	Mean	SD
Tension	Force, N	10	15	25	27	57	63	69	82	100	133	58.1	39.9
	Stress, MPa	1.01	1.52	2.53	2.73	5.76	6.36	6.97	8.28	10.10	13.43	5.87	4.03
	EF area, mm²	—	—	—	—	0.08	—	—	—	0.22	0.27	0.057	0.103
	EF percentage	—	—	—	—	0.8%	—	—	—	2.2%	2.7%	0.57%	—
Shear	Force, N	5	17	44	68	78	80	83	93	163	168	79.9	53.6
	Stress, MPa	0.51	1.72	4.44	6.87	7.88	8.08	8.38	9.39	16.46	16.97	8.07	5.41
	EF area, mm²	—	—	—	—	0.22	—	—	0.24	0.36	0.56	0.138	0.200
	EF percentage	—	—	—	—	2.2%	—	—	2.4%	3.6%	5.6%	1.38%	—
Torsion	Torque, N-mm	60	80	95	100	100	135	150	225	305	345	159.5	98.9
	EF area, mm²	—	—	—	—	0.08	0.19	0.28	0.57	0.75	0.77	0.264	0.317
	EF percentage	—	—	—	—	0.8%	1.9%	2.8%	5.7%	7.5%	7.7%	2.64%	—

[a] A blank cell beneath a specimen indicates that no enamel fracture was found. EF indicates enamel fracture.

where $\{\Delta\sigma_n^i\}$ = stress error vector at node n of element i; $\{\Delta\sigma_n^a\}$ = averaged stress vector at node $n = \sum_{i=1}^{N_e^n} \{\sigma_n^i\}/N_e^n$; N_e^n = number of elements connecting to node n; $\{\sigma_n^i\}$ = stress vector of node n of element i.

Then, for each element,

$$e_i = \frac{1}{2}\int_{\mathrm{vol}} \{\Delta\sigma\}^{\mathrm{T}}[D]^{-1}\{\Delta\sigma\}\ d(\mathrm{vol})$$

where e_i = energy error for element i in the enamel part, vol = volume of element in the enamel part, $[D]$= stress-strain matrix of enamel material, and $\{\Delta\sigma\}$ = stress error vector.

The energy error over the model is as follows:

$$e = \sum_{i=1}^{N_r} e_i$$

where e = energy error over the enamel part, and N_r = number of elements in the enamel part.

$$E = 100\left(\frac{e}{U + e}\right)^{1/2}$$

where E = percentage error in the energy norm, and U = strain energy over the enamel part.

In keeping with the study findings of Zienkiewicz and Zhu,[15] an E value below 10 means that the FEM mesh allows the FEM to achieve acceptable stress values. In this FEM, the E value of the stress evaluated for the enamel was 8.3 in the tension mode, 8.0 in the shear mode, and 8.4 in the torsion mode. These E values confirmed that stress evaluation of the FEM is acceptable.

RESULTS

Tension Mode

SEM examination showed that EFs were found in three specimens (#5, #9, and #10), as is shown in Table 1. The greatest EF area occupied 2.7% of the total bracket area. The EFs were located around the three corners, as is shown in Figure 2A. The FEM indicated high stress at the corners, which matched the results of the SEM examination. The maximum principal stress was 15.67 MPa, as is shown in Figure 2B.

Shear Mode

SEM examination showed that EFs were found in four specimens (#5, #8, #9, and #10), as is shown in Table 1. The largest EF area reached 5.6% of the total bracket area. EFs in the shear mode were most often located on the exerting side and in its nearby regions, as is shown in Figure 3A. FEM simulation indicated that the maximum principal stress reached 55.49 MPa and showed that high stress most often appeared on the force-exerting side, as is shown in Figure 3B. Stress was distributed asymmetrically over the enamel; this matched the SEM results.

Torsion Mode

SEM examination showed that EFs were found in six specimens (#5, #6, #7, #8, #9, and #10), as is shown in Table 1. The largest EF area reached 7.7% of the total bracket area. Figure 4A shows that EFs most often occurred along the exerting edges. Figure 4B shows that the FEM found high stress on the exerting edges, which matches the SEM results. The maximum principal stress reached 43.6 MPa.

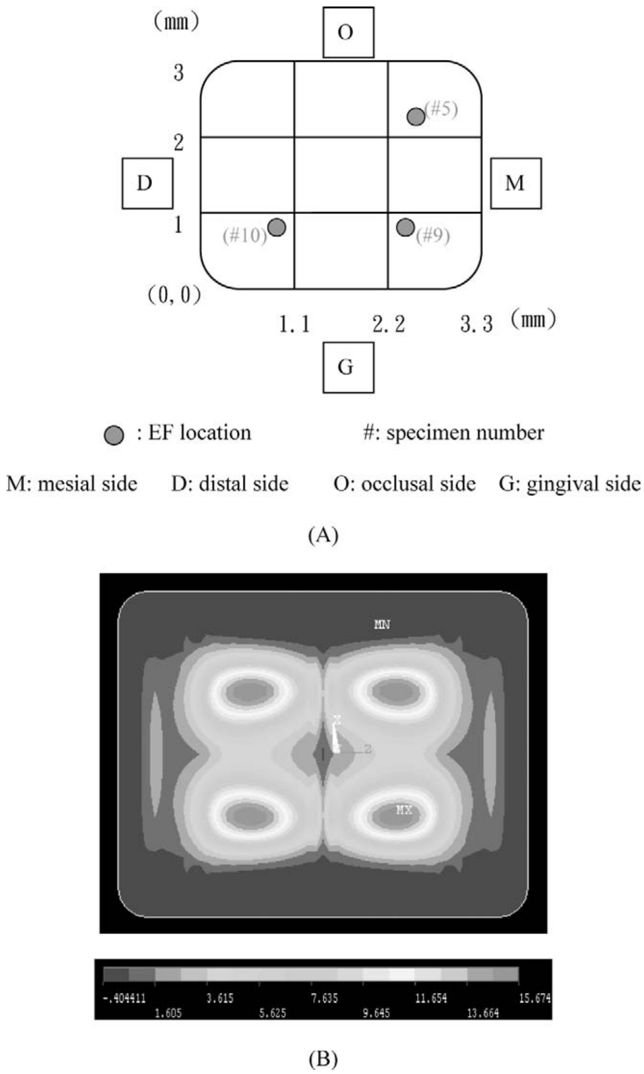

Figure 2. Tension mode: (A) The enamel fracture (EF) location on the debonded enamel surface is itemized by specimen number. (B) The maximum principal stress distribution on the enamel surface (unit: MPa).

Mean debonding loads for the tensile, shear, and torsion forces were 58.1 N, 79.9 N, and 159.5 N-mm, respectively, as is shown in Table 1. In this study, these test loads were regarded as the loading condition in the FEM. The independent *t*-test showed no significant difference between the tensile mode group and the shear mode group ($P = .316$) in terms of the force needed to debond the brackets. Therefore, when an orthodontic bracket is debonded, the choice between tensile and shear force is not critical. Results from torsion failure investigations cannot be compared with those from tension or shear tests. Torsion is expressed in units of Newton-millimeter (N-mm), whereas Newton is the unit of tension and shear forces.

Both the ANOVA test ($P = .347$) and the Kruskal-Wallis test ($P = .244$) showed no significant differences in the size of EFs created through these three loading modes. As to the incidence of enamel fracture, pairwise comparisons with Fisher's exact tests with Bonferroni correction ($P = 1.000$, .370, and .656, respectively) showed no significant differences among the three groups.

DISCUSSION

From the SEM results, it can be seen that the EF location usually occurs in the exerting region for all three loading modes. For example, enamel fracturing occurred along the exerting edges in torsion mode, along the exerting side in shear mode, and around the exerting bracket corners in tension mode. The stress distribution obtained from FEM analysis matched mechanical testing and SEM results well.

From a material mechanics viewpoint, twisting the load in a swirling motion sweeps stress into a spiral motion across the enamel surface, as is shown in Figure 4A, gradually increasing it from the center outward. Thus, we found little stress in the center region, as is shown in Figure 4B. However, the shear mode is different from the torsion mode. The tooth surface is convex in the center region, and shear force is exerted parallel to the side of the tooth surface. Therefore, FEM found that shear stress was likely to start from the exerting side and to stop in the center, that is, stress flow was blocked on the convex side. SEM observations revealed that the distal side contained almost no EF areas. In Figure 2A, the enamel was fractured, usually around the exerting bracket corners in tension mode—a fact that we attribute to force in the vector direction. The tensile force vector was directed away from the enamel surface through the bracket corners, and the concentrated tensile stress fractured the enamel, as is shown in Figure 2B.

With regard to stress calculation from mechanical testing, our study estimated that average tensile stress and average shear stress were 5.9 MPa and 8.1 MPa, respectively. Under the same debonding velocity, a previous study[14] reported that average tensile stress and average shear stress were 6.5 MPa and 10.8 MPa, respectively. In shear mode, different etching times generated some variation, with a range from 9.38 MPa to 12.15 MPa.[9] Thus, our data derived from mechanical testing were not very different from previous results. However, mechanical testing often is criticized for not representing a clinical stress situation realistically.[17] The actual debonding load that simulated hand force required to remove a bracket reached only 5.47 MPa[18]; thus, our mechanical testing loads were actually a little larger than the hand debonding loads used in clinical practice.

Although this study took advantage of SEM, FEM,

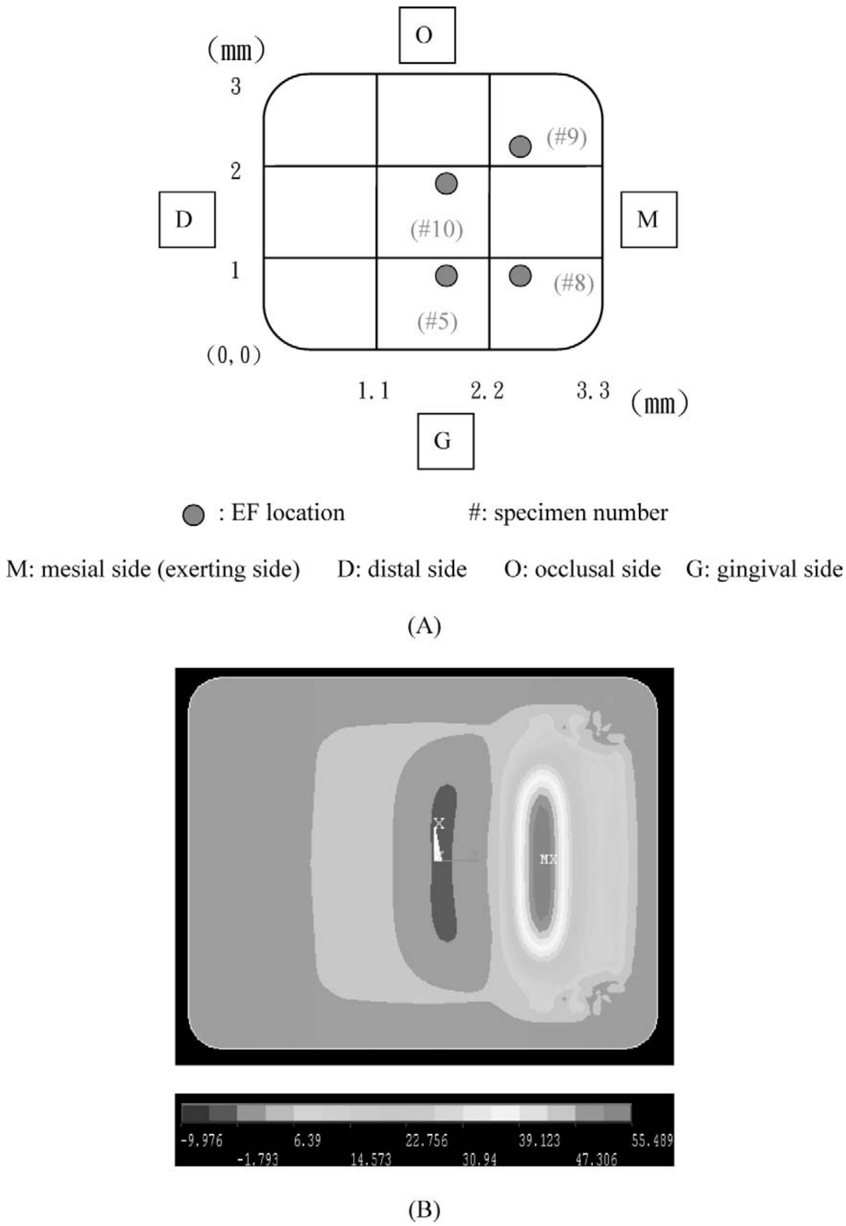

Figure 3. Shear mode: (A) The enamel fracture (EF) location on the debonded enamel surface is itemized by specimen number. (B) The maximum principal stress distribution on the enamel surface (unit: MPa).

and mechanical testing to investigate EFs, certain limitations and assumptions should be noted. The FEM was assumed to be isotropic, homogeneous, and linear elastic. Therefore, the FEM was mainly used to perform a qualitative analysis of stress distribution, and it was used in combination with SEM to identify possible reasons and a tendency prediction for EF after bracket debonding. The stress distribution obtained from the FEM analysis matched the mechanical testing and SEM results well.

In the mechanical tests, the standard deviation was large, which may be due to such factors as varied structural qualities of the enamel, tooth wear, possible cracks in the enamel, or an incomplete curve match between brackets and premolars. Besides enamel failure, other failure types included cohesive/adhesive failure and adhesive failure at the enamel/adhesive interface or at the adhesive/bracket interface. The debonding load result for each stress mode could be very significantly affected by the failure modes. The high standard deviation could be attributed in part to different failure modes. Therefore, these possible reasons for large standard deviations in the mechanical test should be investigated in greater detail in future studies.

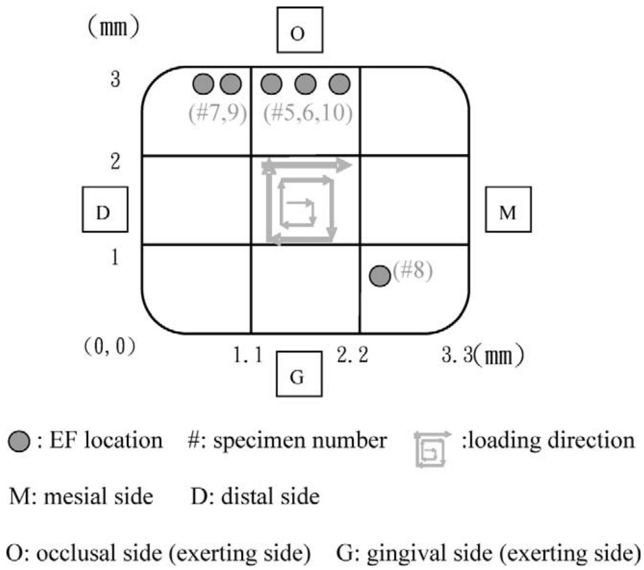

(A)

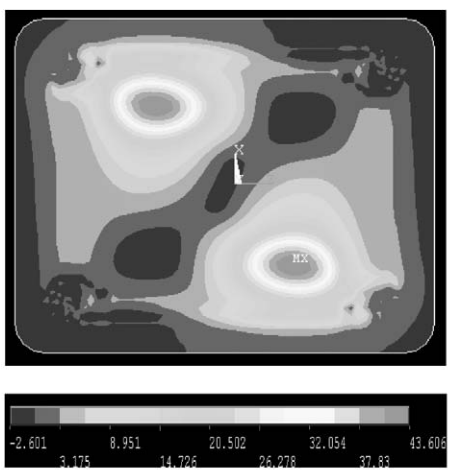

(B)

Figure 4. Torsion mode: (A) The enamel fracture (EF) location on the debonded enamel surface is itemized by specimen number. (B) The maximum principal stress distribution on the enamel surface (unit: MPa).

CONCLUSIONS

- EF locations coincided with the areas where tensile, shear, or torsion force was exerted. On the basis of these results, the dentist must pay extra care and attention to these specific areas of enamel after debonding.
- The sizes and incidences of EF produced by the tensile, shear, or torsion debonding mode showed no significant difference. Thus, clinically, when the sizes and incidences of produced EF are considered, it should not matter which of the three exerting forces is used to debond a bracket.

ACKNOWLEDGMENTS

This research was supported by grant NSC 93-2213-E-010-010 from the National Science Council and by a grant from the Ministry of Education Aim for the Top University Plan.

REFERENCES

1. Meng CL, Li CH, Wang WN. Bond strength with APF applied after acid etching. *Am J Orthod Dentofacial Orthop.* 1998;114:510–513.
2. Sorel O, el Alam R, Chagneau F, Cathelineau G. Changes in the enamel after in vitro debonding of brackets bonded with a modified glass ionomer cement. *Orthod Fr.* 2000;71:155–163.
3. Sorel O, El Alam R, Chagneau F, Cathelineau G. Comparison of bond strength between simple foil mesh and laser-structured base retention brackets. *Am J Orthod Dentofacial Orthop.* 2002;122:260–266.
4. Rossouw PE, Terblanche E. Use of the finite element analysis in assessing stress distribution during de-bonding. *J Clin Orthod.* 1995;29:713–717.
5. DeHoff PH, Anusavice KJ, Wang Z. Three-dimensional finite element analysis of the shear bond test. *Dent Mater.* 1995;11:126–131.
6. Liu JK, Chang LT, Chuang SF, Shieh DB. Shear bond strengths of plastic brackets with a mechanical base. *Angle Orthod.* 2002;72:141–145.
7. Wang WN, Li CH, Chou TH, Wang DDH, Lin LH, Lin CT. Bond strength of various bracket base designs. *Am J Orthod Dentofacial Orthop.* 2004;125:65–70.
8. Knox J, Jones ML, Hubsch P, Middleton J, Kralj B. An evaluation of the stresses generated in a bonded orthodontic attachment by three different load cases using the finite element method of stress analysis. *J Orthod.* 2000;27:39–46.
9. Osorio R, Toledano M, Garcia-Godoy F. Bracket bonding with 15- or 60-second etching and adhesive remaining on enamel after debonding. *Angle Orthod.* 1999;69:45–48.
10. Gung YW, Kuo SM, Wang YJ. Effect of PVA-AA on dentine bonding of HEMA. *Biomaterials.* 1997;18:367–371.
11. Korbmacher H, Huck L, Adam T, Kahl-Nieke B. Evaluation of an antimicrobial and fluoride-releasing self-etching primer on the shear bond strength of orthodontic brackets. *Eur J Orthod.* 2006;28:457–461.
12. Fox AF, McCabe JF, Buckley JG. A critique of bond strength testing in orthodontics. *Br J Orthod.* 1994;21:33–43.
13. Oesterle LJ, Shellhart WC. Bracket bond strength with transillumination of a light-activated orthodontic adhesive. *Angle Orthod.* 2001;71:307–311.
14. Komori A, Ishlkawa H. Evaluation of a resin-reinforced glass ionomer cement for use as an orthodontic bonding agent. *Angle Orthod.* 1997;67:189–196.
15. Zienkiewicz OC, Zhu JZ. A simple error estimator and adaptive procedure for practical engineering analysis. *Int J Numer Methods Eng.* 1987;24:337–357.
16. ANSYS Inc. *Theory Reference Release 7.0.* Houston, Tex: Swanson Analysis System, Inc.; 1999.
17. Eliades G. Clinical relevance of the formulation and testing of dentine bonding system. *J Dent.* 1994;22:73–81.
18. Pickett KL, Sadowsky PL, Jacobson A, Lacefield W. Orthodontic in vivo bond strength: comparison with in vitro results. *Angle Orthod.* 2001;71:141–148.